

A Qualitative Assessment of Microclimatic Perturbations in a Tunnel

Rohit Salve and Michael B. Kowalsky

Earth Sciences Division, Lawrence Berkeley National Laboratory,

1 Cyclotron Road

MS-1116, Berkeley CA 94720

Phone: 510 486 6416

Fax: 510 486 6608

Email: R_Salve@lbl.gov

Abstract

Understanding microclimate dynamics in tunnels is important for designing and maintaining underground facilities. For example, in the geological disposal of radioactive materials, condensation of vapor should be minimized as it can accelerate waste package corrosion and radionuclide release. While microclimate dynamics are known to be dominated by the advection of heat and moisture, additional factors may also be important, such as the presence of fractures or faults. We present a relatively inexpensive method to assess microclimatic perturbations within a tunnel. By combining standard temperature and relative humidity sensors with low-cost sensors designed to detect changes in condensation, we monitored microclimate dynamics along a tunnel at the proposed geological repository at Yucca Mountain, Nevada. We observed significant differences in the pattern of condensation in a faulted zone relative to that of a nonfaulted zone, suggesting that the microclimate dynamics of excavated cavities in fractured, partially saturated rocks can be highly complex.

Key Words

Microclimate, Tunnels, Condensation, Evaporation, Fractured Rock , Monitoring Techniques

28

29 **I. Introduction**

30 An understanding of microclimate dynamics in underground cavities is important for
31 applications ranging from the design of waste disposal facilities to the preservation of
32 artifacts or fauna in caves (de Freitas and Schmekal, 2003). In such environments,
33 typically having high humidity and containing partially saturated rocks, the microclimate
34 is dominated by advection of heat and moisture (De Freitas and Littlejohn, 1987), with
35 the thermal state being defined by the geothermal flux, thermal diffusion from the
36 surface, water circulation, and air exchange with the outside atmosphere (Crouzeix *et al*,
37 2003).

38 At the proposed geological repository for radioactive waste at Yucca Mountain,
39 Nevada, it is crucial to minimize exposure of waste containers emplaced in horizontal
40 tunnels (drifts) to water. The presence of in-drift water caused by seepage from the
41 surrounding rock mass or by condensation of vapor can accelerate waste package
42 corrosion and potentially enhance radionuclide dissolution, release and transport. It is
43 important to understand the microclimates that could develop in this fractured and faulted
44 rock environment, and the subsequent propensity for water condensation.

45 Yucca Mountain is located in the central portion of the southern Basin and Range,
46 which resulted from late Cenozoic extensional faulting (Piety, 1996). Key features in the
47 structural geology of the region include block-bounding faults, occurring every 1–4 km,
48 and intrablock faults (Stuckless and Dudley, 2002). Because the proposed geological
49 repository will include kilometers of horizontal tunnels, it will inevitably be intercepted
50 by sub near-vertical faults.

Here we present a relatively inexpensive technique for monitoring microclimate dynamics along a tunnel. Using sensors designed to detect changes in water saturation caused by condensation and evaporation, we were able to monitor in-drift microclimate dynamics at higher temporal and spatial resolution than previously investigated (to our knowledge). We observed significant differences between and within faulted and nonfaulted zones. The complexity of the microclimate dynamics highlights the need for such studies in designing facilities in fractured, partially saturated rocks.

II. The Study Site

The study was conducted over a period of 14 months, beginning in late 2001, in the immediate vicinity of the Solitario Canyon Fault Zone (SCFZ) at Yucca Mountain (Figure 1). The SCFZ, considered to be the laterally most continuous fault at Yucca Mountain, is accessible ~300 m below ground surface through a 2.7 km long, 5 m diameter tunnel, the Cross Drift (CD). The CD, excavated in 1998, is located entirely within the Topopah Spring Tuff (Figure 1a). The eastern strand of the SCFZ begins at Sta. 25+85, though the influence of the SCFZ on the surrounding rock extends to Sta. 25+00 in the form of shear intensity (Mongano et al., 1999). (“Sta.” indicates station and is followed by distance in meters, with 25+85 indicating, for example, the location 2,585 m from the start of the CD).

III. Methods

a. Isolation of the CD from engineered ventilation

During the six-month excavation of the CD, engineered ventilation was maintained by a series of fans in a ~1 m diameter tube extending over the length of the tunnel which drew air into the tube and transported it out of the tunnel. The impact of the engineered ventilation on the in-drift microclimate and surrounding formation was substantial, and thus had to be mitigated for this investigation, which was accomplished by isolating four sections along the terminal section of the CD with steel doors, referred to as bulkheads, at Sta. 17+63, 22+00, 25+03, and 26+00 (Figure 1b). The first two sections were outside the SCFZ: between Sta. 17+63 and 22+00 (Section 1), and between Sta. 22+00 and 25+03 (Section 2). The third section (Section 3) was located between Sta. 25+03 and 26+00 and included the eastern strand of the Solitario Canyon Fault. The fourth section (Section 4) was located beyond Sta. 26+00 in a faulted zone between the eastern and western strands of the Solitario Canyon Fault. This configuration allowed us to monitor microclimate dynamics outside of (Sections 1 and 2) and within (Sections 3 and 4) the SCFZ.

On November 19, 2001, the ventilation was stopped in Sections 2-4 and these sections were sealed by closing the last three bulkhead doors. One month later Section 1 was similarly sealed by closing the first bulkhead door and removing ventilation. Sections 2-4 would remain sealed for 15 months, while Section 1 would for only 7 months. To remove artificial sources of heat, electrical power to the investigated region was stopped, except for the 12 V batteries used to power the data loggers and sensors.

b. Monitoring of in-drift microclimate in faulted and nonfaulted zones

Humidity and temperature were measured (Model HMP45C, Campbell Scientific Inc.) in the isolated Sections 1–4 of the CD, and just outside the isolated sections (at Sta. 15+00), where engineered ventilation remained active.

Electrical resistance probes (ERPs) were used to monitor changes in condensation along 200 m of the drift at high spatial and temporal resolution. Working under the principle that the water saturation of a material is inversely proportional to the electrical resistance (Archie, 1942; Blasch et al., 2002), Salve et al. (2000) developed ERPs using filter paper as the sensing element, such that the electrical resistance depended on the amount of water adsorbed on the filter paper. Placed close to the floor of the tunnel and exposed to the in-drift atmosphere, a total of 400 ERPs were installed at 0.5 m intervals between stations 24+00 (in Section 2) and 26+00 (at the end of Section 3). To keep water from pooling on or near the probes and influencing subsequent measurements, the ERPs were mounted on the outer curved surface of PVC pipes that were sectioned length-wise.

The measurement system for the ERPs included four data loggers (Model CR10X, Campbell Scientific Inc., Logan, Utah), each connected to several multiplexers (Model A416, Campbell Scientific Inc., Logan, Utah). The data loggers and multiplexers were placed in air-tight containers to prevent corrosion from the humid in-drift air. An internal check of the measurement system was provided with precision resistors placed on the measurement ports of the multiplexers and near some of the ERPs.

The ERP data were compared with data from co-located relative humidity (RH) sensors (Model HMP 45C, Campbell Scientific). The relationship between these two data types is as follows: an increase in relative humidity, as measured by the RH sensor, causes an increase in condensation on (and thus water saturation of) the ERP filter paper, resulting in a decrease in electrical resistance, as measured by the ERPs (and vice versa). Figure 2 compares the ERP and RH response at two locations, focusing on the RH range of 90%–100% (values below this are of less interest as they reflect conditions in which

humidity is unnaturally low due to the engineered ventilation). The relationship between the two data types is as expected, with decreasing electrical resistance closely tracking the increasing RH.

IV. Observations

a. Temperature and relative humidity

The temperature and RH measurements for Sections 1–4 are presented in Figure 3. When ventilation was removed from Sections 2–4 in mid-November 2001, there was an immediate, rapid decrease in temperature that persisted for ~1 week, followed by a gradual decrease (Figure 3a). While the temperature was slightly higher (relative to Sections 2–4) in Section 1, (this section was not isolated from ventilation effects until the third week in December 2001), the pattern was similar as for the other sections. When the first bulkhead door was opened in June 2002, the temperature in Section 1 immediately increased. A more gradual increase was observed in Section 2 (measured at Sta. 23+45) over the next five months. Temperatures in Section 4 (measured at Station 26+30) consistently remained higher than in Sections 2 and 3 until November 2002, when some sensors failed.

RH measurements show that humidity in the four nonventilated sections began to increase after the bulkhead doors were closed and ventilation was stopped (Figure 3b). Similar to the temperature responses, there was an initial period of rapid change in RH, followed by a slower rise after the first few weeks. In Section 1 (at Sta. 21+40), after the section was sealed in December 2001, there were initially rapid changes in over a period of two weeks, with values rising from ~10 to ~90%. In the following 5 months, the RH

continued to rise, but was interrupted at weekly intervals, likely affected by the adjacent non-isolated section of the drift, for which ventilation was active from Monday through Thursday and inactive from Friday through Sunday of each week. Deeper in the CD (in Sections 2–4), the average RH response was almost identical in each section, with the RH increasing rapidly to ~90% and then gradually toward 100%. The periodic disruptions in RH observed in Section 1 were not observed in Sections 2–4.

Note that we observed no correlation between the barometric pressure (not shown) and the temperature and RH data.

b. Electrical resistance probes (ERPs)

After the engineered ventilation was removed, ERP resistance values began to rapidly decrease for a few months before reaching a relatively constant value (Figure 4a). The decrease in the nonfaulted zone (Sta. 24+00 to 25+00) was generally faster than in the faulted zone (Sta. 25+00 to Sta. 26+00). After the initial decrease, the resistance in the nonfaulted zone remained mostly uniform at low values (i.e., indicating wetter conditions with more condensation) compared to the faulted section with increasingly higher values (i.e., indicating drier conditions with less condensation).

Within the nonfaulted section, small differences in the general pattern were noted between January and August 2002, when the region between Sta. 24+00 and 24+20 remained drier than the rest of the nonfaulted zone. By September 2002, these differences disappeared, but others began to emerge. For example near Sta. 24+35, there was a large decrease over several meters which persisted until the end of monitoring. However, for

the remainder of this section (Sta. 24+40 to 25+00) the response was relatively uniform following the initial decrease.

As in the nonfaulted section, there was no identifiable spatial trend in the faulted section during the first few months. However, by April 2002, for a period of about two months, the faulted section shows a trend going from lower to higher resistance (higher to lower condensation) with increasing station number. This spatial pattern was interrupted in early July 2002, when a substantially wetter zone developed abruptly between Sta. 25+65 and 25+75.

It is interesting to note that the sharp contrast in resistance on either side of the bulkhead door at Sta. 25+03 suggests that the bulkhead door likely influenced the microclimate in its vicinity.

The resistance profile is shown in Figure 4b for two times during the monitoring period. Note that for the earlier time the spatial fluctuations are relatively minor, and a trend of increasing resistance is seen in the faulted zone (Sta. 25+00 to 26+00). While the later profile shows similarly mild fluctuations in the nonfaulted zone (except near Sta. 24+35), more extreme fluctuations are seen in the faulted zone.

c. Precision resistors

Measurements were also collected using standard resistors, referred to here as “precision resistors,” to check that the measurement systems were functioning properly (i.e., the resistance measured across these resistors was expected to remain constant and be unaffected by the surroundings). An interesting, though unexpected observation was made when changes were detected in the precision resistors.

Some of the precision resistors were placed in sealed containers and isolated from the in-drift microclimates, while the rest were located alongside ERPs and thus were exposed to the in-drift microclimates. The isolated resistors showed no significant changes during the investigation (Figure 5a). However, the resistors exposed to the in-drift conditions showed substantial changes that were similar in nature (but smaller in magnitude) to the changes observed in the ERP data, with slightly less variability in the nonfaulted zone (Figure 5b) than in the faulted zone (Figure 5c). It appears that the high humidity conditions within the drift resulted in condensation that caused steady but non-uniform corrosion of the precision resistors.

V. Discussion and Conclusion

When engineered ventilation is suppressed in excavated cavities that are thought to be isolated from atmospheric dynamics, it is tempting to assume that a low-energy environment with a stable internal microclimate exists (e.g., Freitas and Littlejohn, 1987; Gamble et al., 2000). However, our observations suggest that in cavities located in fractured/faulted rock, such as the CD at Yucca Mountain, the microclimatic regime is dynamic and may vary unexpectedly from the assumed low-energy environment.

The following observations can be made from this study:

1. The ERP response suggests that there are changes in condensation patterns within the drift over the large spatial scale (200 m) and long time frame (~14 months) that we examine. Some areas of the drift are subject to greater amounts of condensation than others.

- 209 2. There are significant differences in the microclimates of the faulted and
210 nonfaulted sections, with the faulted section showing greater variability.
- 211 3. Non-uniform corrosion of precision resistors (installed with the intent of
212 providing a check on the electronics) also suggests spatial variability in the in-
213 drift moisture dynamics.

214

215 While qualitative in nature—since we based our observations on trends seen in a
216 large number of ERPs that were not calibrated specifically to provide condensation or RH
217 estimates—the results of this study point to the need for detailed, quantitative
218 investigations of in-drift microclimates for designing or maintaining facilities in
219 fractured, partially saturated rocks.

221 **Acknowledgments**

222 This work was supported by the Director, Office of Civilian Radioactive Waste
223 Management, U.S. Department of Energy, through Memorandum Purchase Order QA-
224 B004220RB3X between Bechtel SAIC Company, LLC, and the Ernest Orlando
225 Lawrence Berkeley National Laboratory (Berkeley Lab). The support is provided to
226 Berkeley Lab through the U.S. Department of Energy Contract No. DE-AC03. Reviews
227 by Stefan Finsterle, Paul Cook, and Dan Hawkes are gratefully acknowledged.

229 **References**

230 Archie GE. 1942. The electrical resistivity log as an aid in determining some reservoir
231 characteristics, *Trans. AIME* 146:54–62.

232 Blasch KW, Ferre TPA, Christensen AH, Hoffmann JP. 2002. New field method to
 233 determine streamflow timing using electrical resistance sensors, *Vadose Zone J.*,
 234 1: 289–299.

235 Crouzeix C, Le Mouél JL, Perrier F, Richon P, Morat P. 2003. Long-term thermal
 236 evolution and effect of low power heating in an underground quarry, *Comptes*
 237 *Rendus Geoscience*, 335: 345–354.

238 De Freitas CR, Littlejohn RN. 1987. Cave Climate: Assessment of heat and moisture
 239 exchange, *J. of Climatology*, 7: 553–569

240 De Freitas CR, Schmekal A. 2003. Condensation as a microclimate process:
 241 measurement, numerical simulation and prediction in the Glowworm Cave, New
 242 Zealand, *Int. J. Climatol.* 23: 557–575.

243 Mongano GS, Singleton WL, Moyer TC, Beason SC, Eatman GLW, Albin AL, Lung RC.
 244 1999. Geology of the ECRB Cross Drift-Exploratory Studies Facility, Yucca
 245 Mountain Project, Yucca Mountain, Nevada, Bureau of Reclamation and U.S.
 246 Geological Survey, Denver, Colorado.

247 Piety LA. 1996. Compilation of known or suspected Quaternary faults within 100 km of
 248 Yucca Mountain, OF 94-0112, USGS, Denver, CO.

249 Salve R., Wang JSY, Tokunaga TK. 2000. A probe for measuring wetting front
 250 migration in rocks, *Water Resour. Res.*, 36: 1359–1367.

251 Stuckless JS, Dudley WW. 2002. The geohydrologic setting of Yucca Mountain, Nevada,
 252 *Appl. Chem.*, 17: 659–682.

253
 254

254 **Figure Captions**

255 Figure 1. (a) Cross section of Yucca Mountain showing the geology of the formation
256 surrounding the Cross-Drift (CD). (b) Location of the four bulkhead doors used to isolate
257 sections of the drift from engineered ventilation. (c) Photograph of the Solitario Canyon
258 Fault in Section 3.

259 Figure 2. Comparison of in-drift electrical resistance probe (ERP) measurements with
260 relative humidity measurements made using commercially available probes (Model HMP
261 45C, Campbell Scientific). The insets depict expanded views over a time period of two
262 weeks.

263 Figure 3. (a) Temperature and (b) relative humidity measured at four locations in the CD.
264 The legend indicates the locations of the sensors along the drift. A drop in temperature
265 after December 6, 2002 in stations 23+45 and 25+55 results from the battery losing
266 adequate power.

267 Figure 4. Resistance measurements collected with ERPs from Sta. 24+00 to 26+00. (a)
268 Data collected at all times with color representing resistance (in $k\Omega$). (b) Resistance
269 profile at two times, as indicated by dashed lines in (a).

270 Figure 5. Precision resistor measurements (a) isolated in sealed containers, (b) open to the
271 in-drift atmosphere in the nonfaulted section, and (c) open to the in-drift atmosphere in
272 the faulted section.

Figure 1.

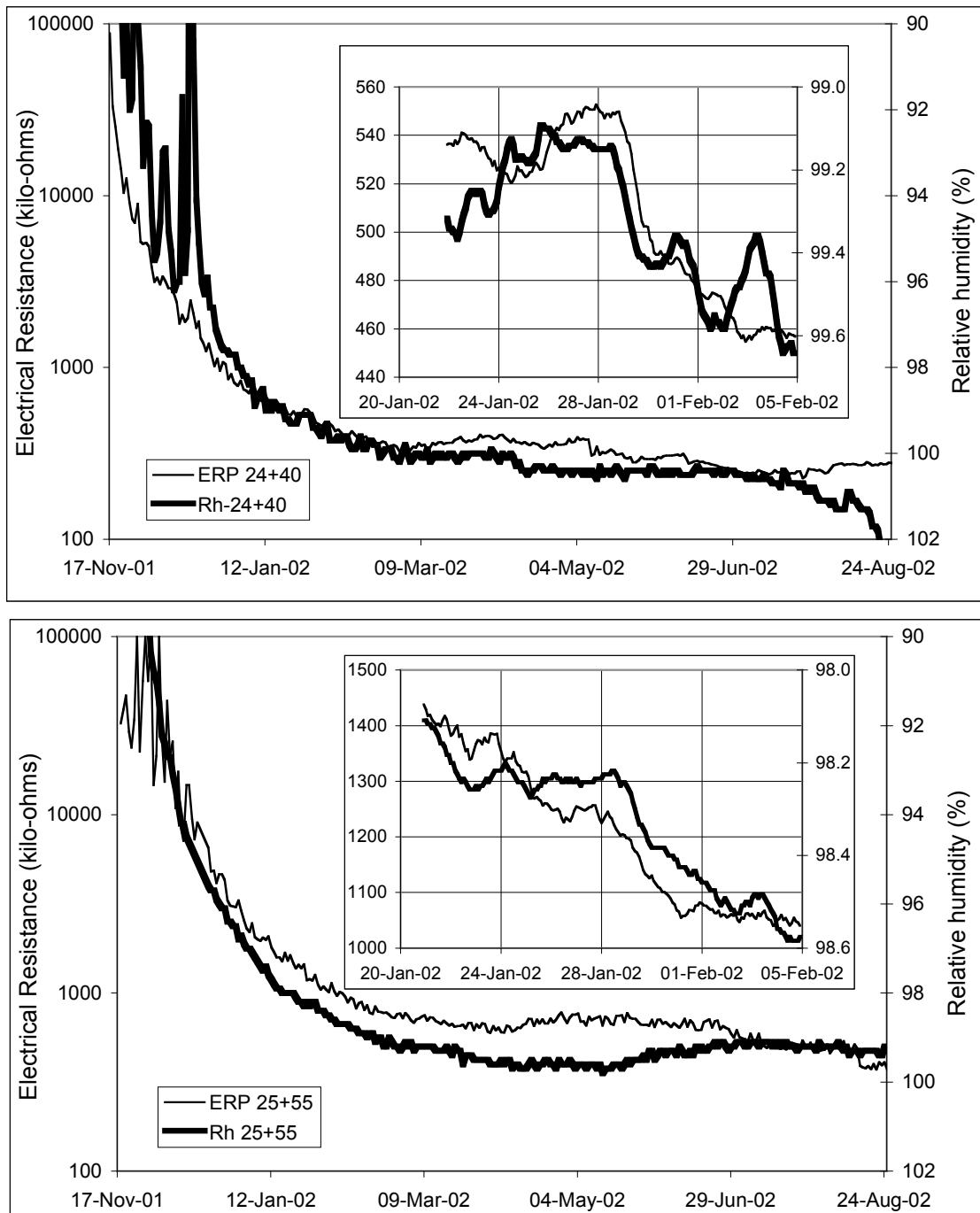


Figure 2.

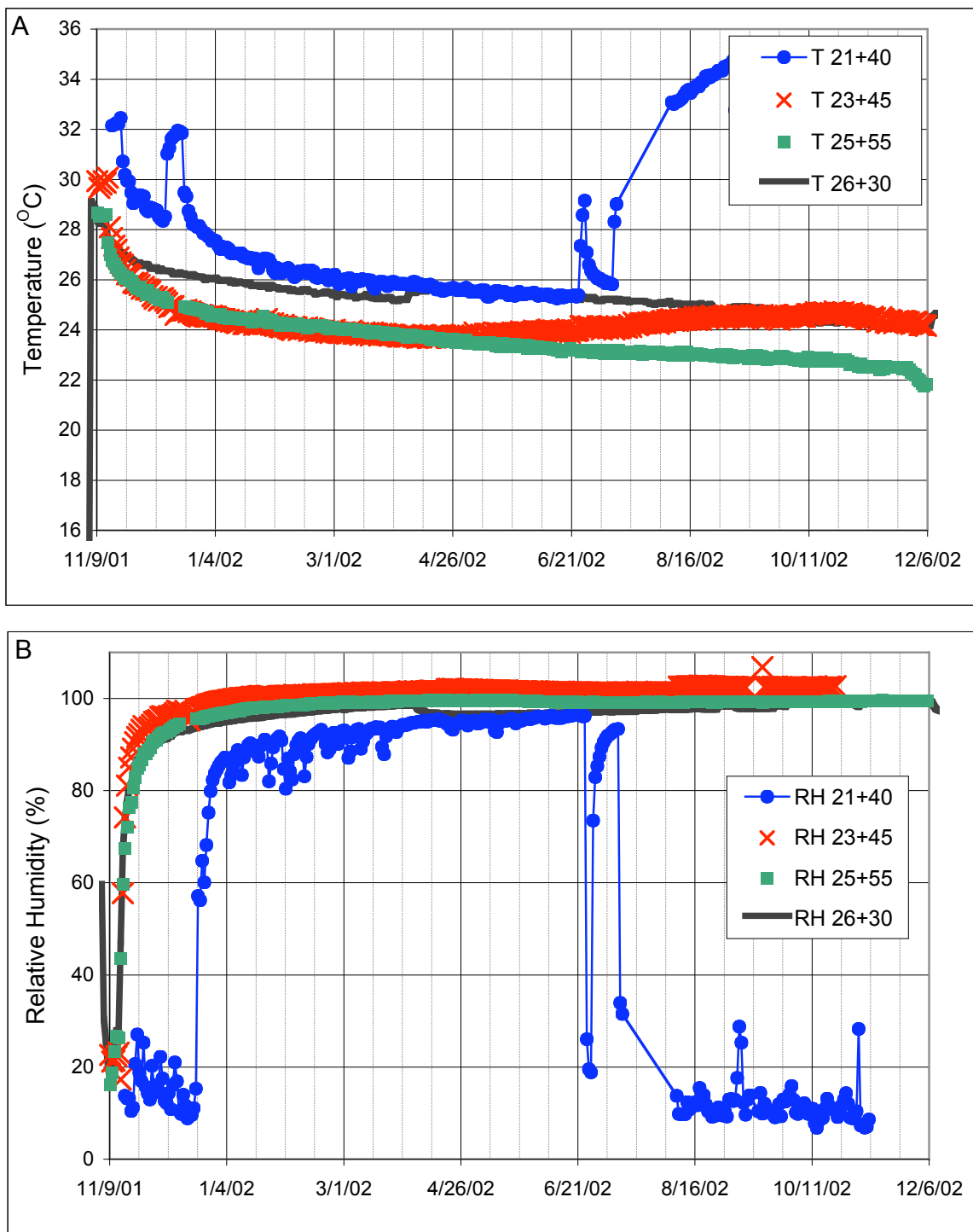


Figure 3.

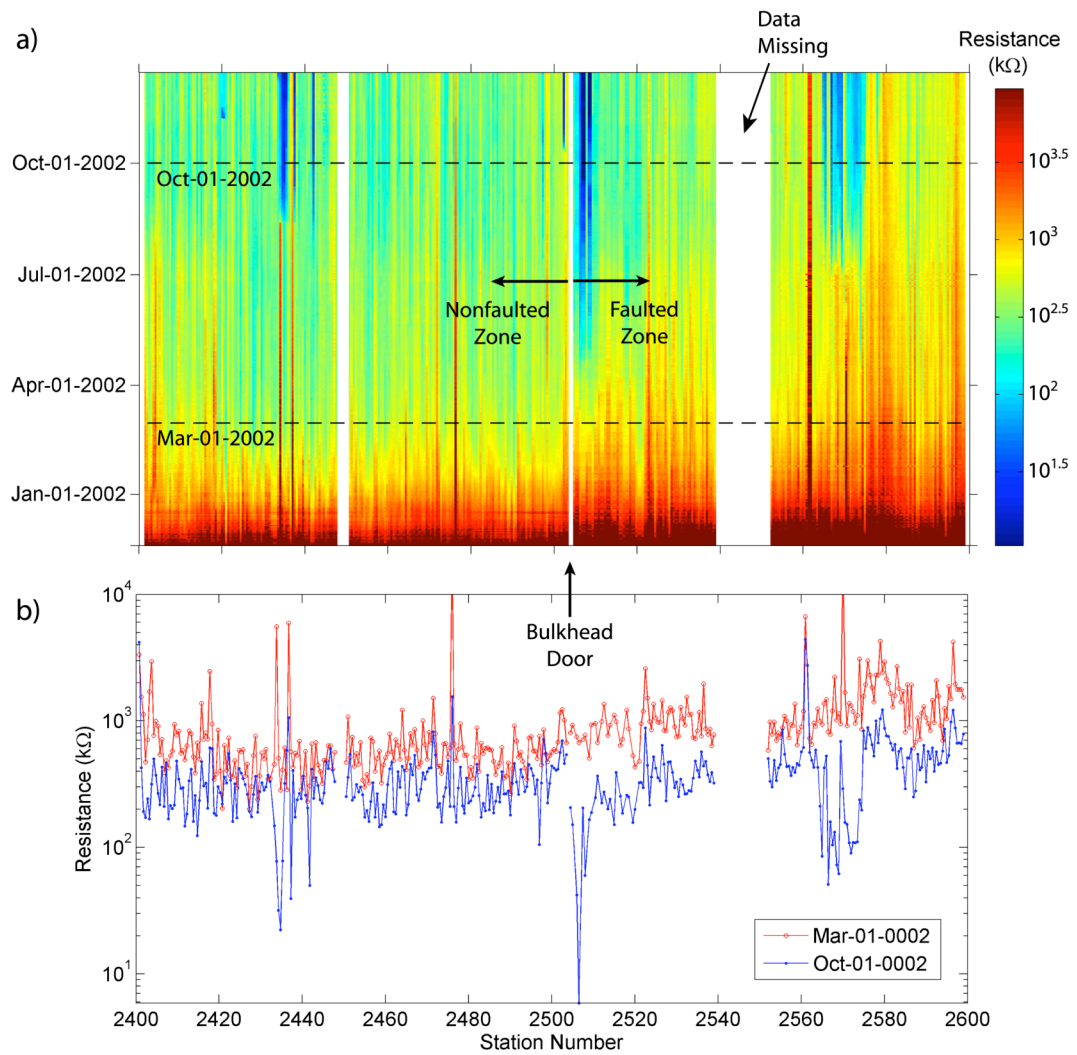


Figure 4.

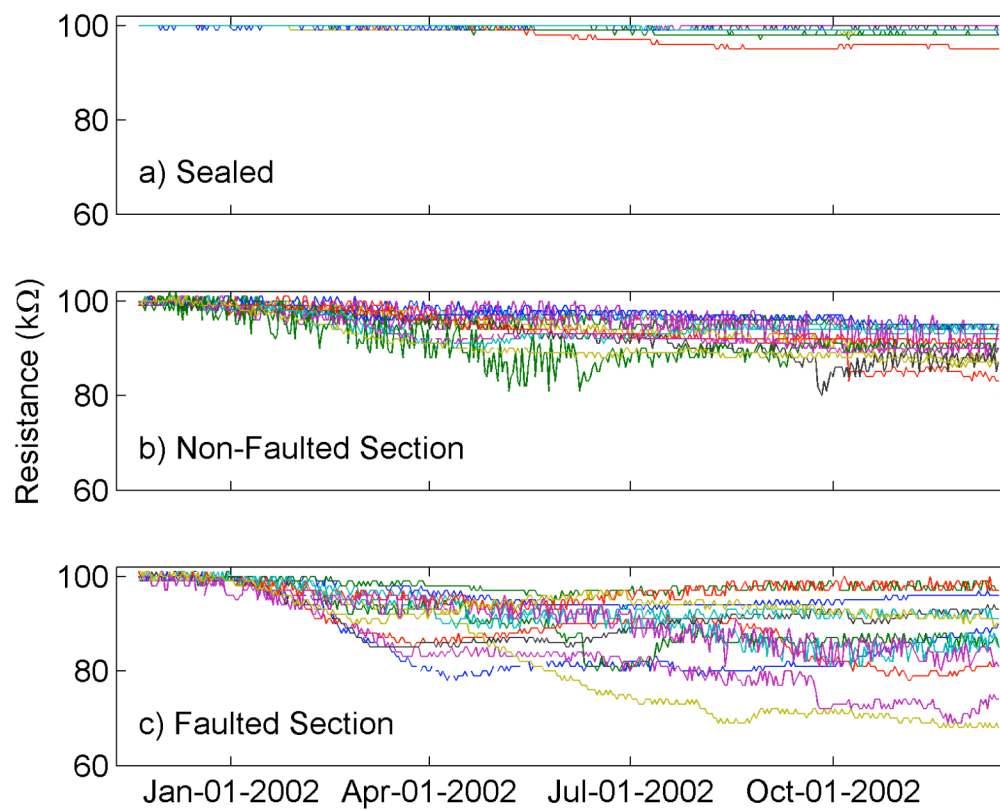


Figure 5.